Use of the Self-Potential Method for Measurement of Subsurface Water Flow at a Pump-and-Treat Remediation Site

By
Danny Fain

Submitted to the Department of Earth, Atmospheric, and Planetary Sciences
In Partial Fulfillment of the Requirements for the Degree of

Bachelor of Science
in Geoscience

at the

Massachusetts Institute of Technology

June, 1999

Signature of Author .....
Department of Earth, Atmospheric, and Planetary Sciences
May 25, 1999

Certified by .....
Frank Dale Morgan
Professor of Geophysics
Department of Earth, Atmospheric, and Planetary Sciences
Thesis Supervisor

Accepted by .....
Ronald G. Prinn
Head of Department
Department of Earth, Atmospheric, and Planetary Sciences

ACKNOWLEDGMENTS

I would like to express my deep gratitude to the following people:

Prof. Dale Morgan, for taking me on as a student, teaching me some of the fundamental concepts of environmental geophysics, directing the course of my investigation, gently guiding my preparation and analysis of the results, and generously spending hours of discussion in helping me to shape the finished product. Without his patient and expert coaching, this thesis would not have been possible.

Yervant Vichabian, for introducing me to the SP technique and equipment, teaching me the subtle craft of electrode preparation, organizing, managing, and doing much of the legwork of the MMR surveys, and helping me to interpret the collected data. His tireless dedication was inspiring; the effort and attention he invested in this project were instrumental to its completion.

John Sogade, for my first hands-on lesson in SP fieldwork, taking part in the MMR survey described in this thesis, and cheerfully helping me with data interpretation and modeling.

Philip Reppert, for providing me with some of the software tools I needed for analysis, and for teaching me the math behind streaming potentials.

Bob Davis, Jerry Galant and Rose Forbes at the MMR IRP, for their help with the logistics and flow management needed for this survey, and for always promptly providing requested information.

Sue Turbak and Liz Henderson, for their help in procuring equipment and supplies, tracking down people, and other logistical support at ERL.

Andrea Parent, for generously donating her time and effort to prepare several of the figures used in this thesis, and for her encouragement and support.

Last but not least, I thank my parents for their love, support, and encouragement over the years.

Table of Contents

List of Figures

1 INTRODUCTION

The self-potential method (SP) of geophysical surveying has been widely used in environmental and engineering applications, primarily for rough but inexpensive assessment of subsurface flow of fluids, heat, or ions. In this project, the SP method was employed to study the activity at an environmental cleanup site at the Massachusetts Military Reservation. At the leading (downgradient) edge of the CS-4 groundwater contamination plume, a fence of pump-and-treat extraction wells has been operating in an effort to contain the plume migration. To help gauge the effectiveness of the pump-and-treat technique, it is useful to delineate the resultant water flow and to compare it to the extent and diffusion gradient of the contaminant plume.

In the survey conducted for this project, SP measurements were taken along the fence of extraction wells, while they were in operation, and during a period in which the well pumps were shut off. Spatial and temporal variations in the SP measurements are analyzed. Some possible explanations are proposed to account for the observed features and changes over time. While the results are not entirely conclusive, they suggest that water flow provides only a modest contribution to the total observed SP anomaly.

2 SITE OVERVIEW

2.1 Background and Contamination History

Area of Contamination Chemical Spill 4 (AOC CS-4) is located at the southern boundary of the Massachusetts Military Reservation (MMR) on Cape Cod, Massachusetts (Figure 2-1). The area at the site's northern end was used for military vehicle maintenance, by the U.S. Army from 1940 to 1946, and by the U.S. Air Force from 1955 to 1973. In addition to motor pool activities, the area was used as a storage yard from 1965 to 1983. Waste products transported to or stored at CS-4 included waste oils, solvents, waste fuels, antifreeze, battery electrolytes, and paint; many of these products were potentially spilled or dumped.

From 1986 to 1990, a series of environmental investigations was conducted at the site by E.C. Jordan Co. (now ABB Environmental Service, Inc.) under contract to Martin Marietta Energy Systems and the U.S. Dept. of Defense Installation Restoration Program. The investigations included site inspections, monitoring wells downgradient of the contamination source, and an aquifer pumping test. The studies concluded that soil in the source area, and groundwater extending downgradient from the source area, were contaminated with volatile organic compounds, primarily 1,2-DCE, PCE, 1,1,2,2-TCA and TCE. The level of contamination was found to be near 100 ppb, while the safe drinking water standard for each is 5 ppb. CS-4 and other contamination sites at MMR are currently on the EPA "Superfund" national priority list of hazardous waste sites. Together, the MMR contamination sites constitute one of the largest toxic waste cleanup sites in the country (Mackay, 1989).

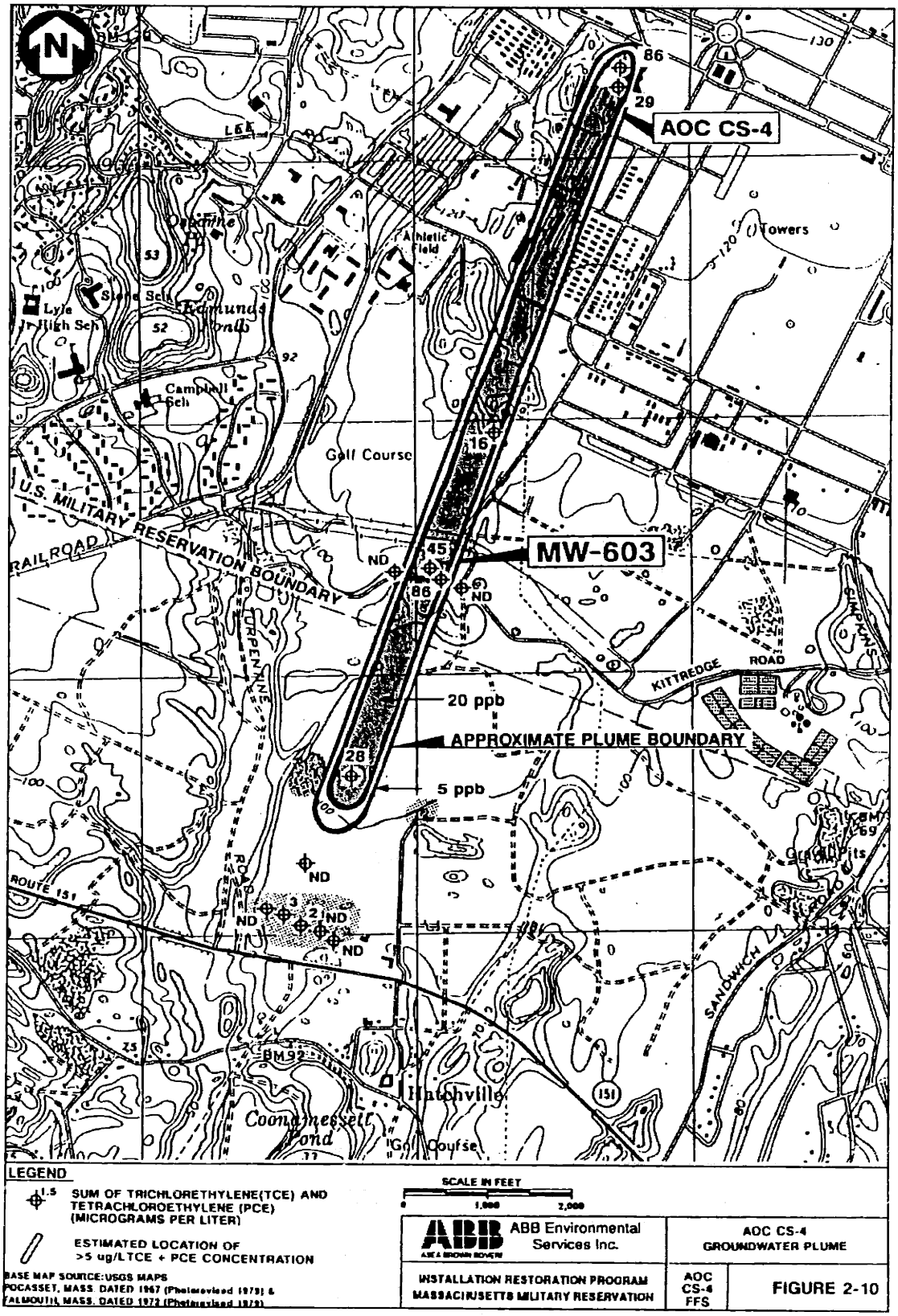

Figure 2-1: Location of CS-4 contamination plume

2.2 Site Geography, Geology, and Hydrology

The southern region of the MMR lies within a broad, southward-sloping glacial outwash plain, termed the Mashpee Pitted Plain (MPP); it is characterized by low topographic relief and an abundance of kettle-hole ponds and marshes (Vichabian, 1997). Located nearby is the Sagamore lens, the sole water-supply aquifer for western Cape Cod; as such, it is of vital importance to four towns adjacent to the MMR: Falmouth, Mashpee, Sandwich, and Bourne.

The MPP consists primarily of highly permeable sand and gravel, and local lenses of less permeable fine-grained silt and clay. The top 2-5 ft (0.5-1.5m) are predominantly a zone of surface soil and weathered residuum, including silty clay, fine sand, and organic matter. Below this layer lie unconsolidated strata of sand, and minor amounts of gravel. Poorly-graded, medium- to coarse-grained sand is interspersed with well-graded gravel. Below 130 ft (40m), dense intervals of fine-grained sediments have been found, with typical thicknesses of 20-25 ft (6-7.5m).

Studies have found that the aquifer within these sands and gravels contains a groundwater contamination plume, originating at the AOC CS-4 source and extending south-southwest beyond the MMR boundary toward Route 151, into the Crane Wildlife Management Area (see Figure 2-1). The sediment porosity is 30%. Contaminant concentrations exceeded a minimum health safety level in a region approximately 11,000 ft (3.35 km) long. At its leading (downgradient) edge, the plume was found to have a cross-section approximately 800 ft (244m) wide and 40 ft (12m) thick. The hydraulic conductivity is about 160 ft/day (49 m/day), the average transmissivity is 20,400 ft^2/day (1900 m^2/day), and the hydraulic gradient is 0.0019 ft/ft; these parameters suggest that the leading edge of the plume is migrating at approximately 370 ft/year (113 m/yr). At the downgradient edge, the estimated depth to the plume is 85 ft (26m).

2.3 Current Remediation Effort

The primary focus of the current remediation effort is containment of the plume at its downgradient edge. A fence of 13 vertical pump-and-treat extraction wells was installed cross-gradient at the plume toe, in the Francis Crane Wildlife Management Area. The wells have been operating since November 1993. Currently, 4 of the wells are inactive due to malfunction; of the remaining active wells, 2 are pumping at 20 gal/min, and 7 are pumping at 15 gpm, for a total throughput of 145 gpm (9.15e-3 m^3/s).

A cross-sectional diagram of each well is shown in Figure 2-1. The intake screen is at a depth of 128-138 ft (39-42m). The pump provides a suction pressure rated at 287 ft dynamic head (8.7 bars). Out of each well, contaminated water is piped to a piping vault located near the center of the well fence (see Figure 4-1); from there, the effluent is piped northward to a treatment facility on the MMR grounds. After chemical treatment, the clean water is discharged upgradient of the plume.

While the pump-and-treat technique is often an effective containment method, its use for lowering of contaminant concentrations can take many decades, due to factors such as sorptive uptake and slow diffusion rates (Mackay, 1989).

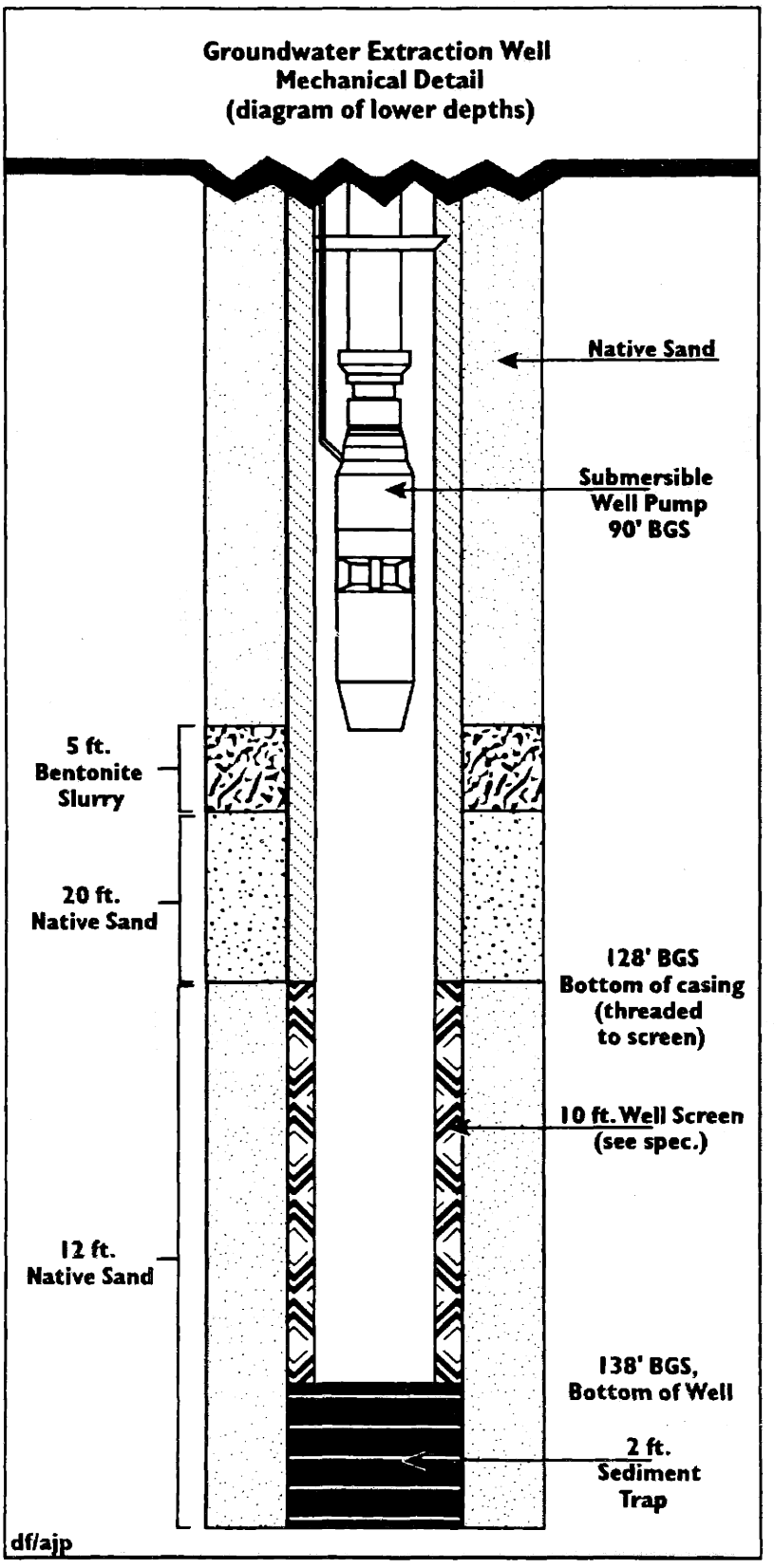

Figure 2-1: Cross-section of extraction well. (Source: MMR IRP)

3 MEASUREMENT METHODS

3.1 Self-Potential Theory and Applications

Self-potential (SP) in geophysical exploration refers to electrical potential differences observed in the ground, due to a naturally occurring (i.e. not purposefully induced) current. SP anomalies are generated by flows of fluid (electrokinetic), heat (thermoelectric), or ions (electrochemical) in the earth; SP investigations have been used to locate and delineate sources associated with such flows (Corwin, 1990). First used for mineral exploration, SP has recently become popular in geothermal, engineering, and environmental applications. Because this method allows rapid field data acquisition, it is cost effective for initial investigation of a site prior to use of more intensive geophysical techniques.

The major environmental application of the SP method has been investigation of subsurface water movement, which is also the subject of interest of this thesis. Water flowing through a porous medium generates an electrokinetic, or "streaming", potential. The theoretical basis of this mechanism was first developed by Helmholtz (Overbeek, 1952). He proposed that preferential transport of positive ions in the fluid through pore capillaries gives rise to an advection current, which is balanced by a conduction current of negative charge in the opposite direction. As positive ions are carried in the direction of water flow, areas of water inflow show a positive SP anomaly, while flow sources show a negative anomaly. In a uniform permeable medium, the streaming potentials show the contours of groundwater flow (Vichabian, grant proposal in preparation).

Another relevant source of self-potential anomalies is electrochemical diffusion potentials. In a chemical transition zone (e.g. the boundary of a contaminant plume), a difference in oxidation potential may exist: one end being relatively reduced, the other end being relatively oxidized. An exchange of ions through pore fluids is balanced by a flow of electrons (from the oxidation site to the reduction site), producing a current that may cause a measurable SP at the surface.

3.2 Electrode Composition and Preparation

The basic equipment required for SP data collection is very simple: a pair of electrodes connected by wire to a measuring device (e.g. voltmeter). However, selection and preparation of materials used in the electrode can greatly affect data quality, which is of particular concern when the studied signal level is low, e.g. tens of millivolts. Laboratory and field studies have shown that liquid-junction electrodes yield fairly reliable data. Such electrodes consist of a metal element immersed in a saturated solution of metal salt, with a porous junction forming the boundary between the solution and the soil (Corwin,1990).

Electrode data quality primarily depends on the polarization and drift characteristics of the electrode pair. Polarization is the potential measured at a specific time between the electrodes in the absence of external electric fields; drift is the time variation of the polarization value. Commercial silver – silver chloride electrodes have been found to provide SP field data of acceptable quality if polarization and drift are monitored; their responses to environmental variations (temperature and soil moisture content) are well-

documented and insignificant in typical applications. Recent experience with custom-assembled silver – sodium chloride electrodes has shown similar characteristics. Accordingly, electrodes of the latter type were chosen for this investigation.

Due to time constraints, new materials could not be obtained in time to assemble fresh electrodes. Therefore, a supply of previously-used electrodes was used. Figure 3-1 shows a cross-sectional view of the electrode. The cylindrical ceramic cups used as the electrode containers had a height of 75-90 mm, a diameter of 35-40 mm, and a porosity of 38%. All of the cups showed varying degrees of wear, including some chipping and cracks, which may have caused excessive leakage of the electrolyte solution; however, this was judged not to be a problem for the 2-3 day period of the survey. The silver wire mesh of some of the electrodes showed signs of oxidation, which undoubtedly contributed to higher-than-optimal polarization values.

In preparing each electrode, the cup was first carefully washed with tap water, then nearly filled with a saturated solution of NaCl in distilled water; the stopper/tubing/silver assembly was fitted into place, and sealed with electrical insulation tape. After preparation, each electrode was visually inspected for leakage, then partly immersed in an upright position in a shallow pan of tap water, with other electrodes. The electrodes' polarizations were measured in pairs, using a hand-held voltmeter, at several intervals (to assess drift). One electrode, common to several pairs having low relative polarization and drift, was selected as the "reference" electrode for the survey. Polarization measurements in this way were performed on April 11 and 12, immediately preceding the survey. Nineteen electrodes were found to have minimally acceptable polarizations (<5 mV) and drift (<1 mV/day) relative to the reference electrode; they were labeled "A"-"S", using a piece of masking tape on the outside of the cup. Table 3-1 shows the polarization of each electrode, as measured on April 12.

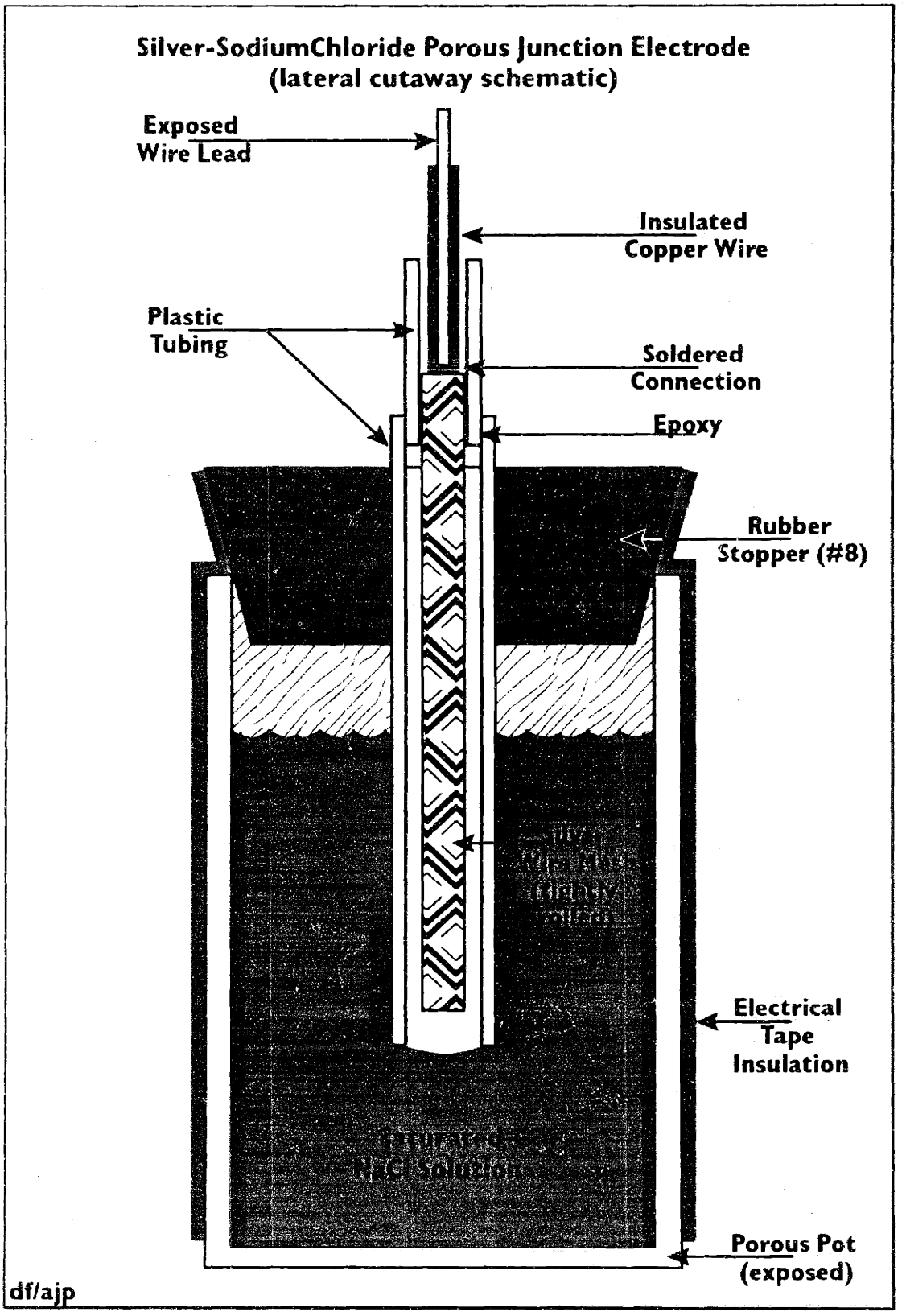

Figure 3-1: Cross-section of electrode

Table 3-1: Electrode initial polarizations and locations in survey array

Electrode	Polarization (mV)	Survey station
A	2.2	16
B	-2.3	14
C	-4.9	1
D	-4.7	15
E	-2.8	8
F	-2.4	18
G	-0.1	3
H	-0.7	7
I	-0.3	13
J	1.6	4
K	2.4	10
L	2.4	17
M	2.4	12
N	2.2	6
O	2.2	2
P	1.0	5
Q	0.0	11
R	2.4	9
S	2.4	Not used

3.3 Survey Configuration

Various electrode configurations can be used in SP surveys, according to the survey objectives, equipment/staffing limitations, and site characteristics. A multi-electrode array configuration was chosen, to permit easy monitoring of both spatial and temporal variations, across the site and throughout the survey day. Other advantages of this configuration are the ability to minimize cumulative error by the use of a single reference station, and application of stacking and filtering techniques to remove undesired temporal noise effects. Disadvantages of this configuration include high initial equipment cost and setup effort; inflexibility in arrangement and spacing of stations over the course of the survey; and logistical difficulty in measuring initial and final electrode polarization values, for correction of polarization errors (Corwin, 1990).

In previous surveys at this site, an SP anomaly was found to span at least 300m along the line of extraction wells; the transverse extent of this anomaly had not been measured yet. An optimal configuration for this survey, given enough electrodes, wire, manpower, and setup time, would have consisted of two perpendicular lines of stations, perhaps 400m and 200m long, intersecting near the center of the well fence. However, a spacing of no more than 20m between stations was judged necessary to ensure sufficient resolution of the anomaly features; such a configuration would have required 30 electrodes. Given the limit of 20 useable electrodes, the two-dimensional array idea was abandoned, and a single ~400m line of stations was judged sufficient.

For signal transmission from each electrode station to the operations base (where the signal measurement was performed), 12 gauge stranded (jacketed) wire was laid out on the ground. For several of the longest runs, two or more pieces of wire were spliced together. Each transmission wire was connected to its electrode by either a weave splice or a short cord with alligator-clip connectors. Any exposed metal was covered with electrical insulation tape, to avoid accidental grounding.

3.4 Voltage Measurement

At the monitoring base (next to the well control vault), the transmission wire ends were connected to the terminal posts of a tie-in block. The terminal posts were also wired to the input channels of an automated data-acquisition system (DAQ), which was in use during the survey; however, technical problems rendered the DAQ-collected data unusable. Throughout the survey, the electrode voltages were manually measured and recorded using a handheld digital multimeter (DMM), a standard commercial model featuring an input voltage range of ±4 V, resolution of 0.1 mV, and input impedance of approximately 10^7 ohm. Readings were taken at the tie-in block, by connecting the negative input to the reference-electrode terminal, and the positive input to the terminal of each measurement electrode in turn.

4 DATA COLLECTION

4.1 Equipment Setup

Equipment setup at the site began around midday on April 13. The weather conditions were quite favorable: partly cloudy, temperature around 50 degrees, with an intermittent gentle to moderate breeze; no rain in the forecast for the next 48 hours. The topsoil was sufficiently moist for adequate electrode contact.

A relatively straight line of electrode stations was laid out along, and extending beyond, the line of extraction wells, in a generally east-west orientation (see Figure 4-1). Nineteen shallow (3-6 inches depth) holes were dug at 20m intervals, for a total survey line length of 360m. The interval spacing was measured using a spooled tape measure; slight deviations, due to natural obstacles (bushes, trees) or ground surface irregularity, led to estimated average measurement error in the range of 5%. The station holes were numbered starting from the western end of the line, while the extraction wells are numbered from the eastern end. Station hole #1 was situated 60m west of extraction well #13 (the westernmost one). The spacing between station holes was slightly greater than between wells (60ft); a few positional coincidences were noted: hole 4 adjacent to well 13; hole 6 adjacent to well 11; hole 15 adjacent to well 1.

One electrode was placed in each station hole, with the reference electrode at hole 1; see Table 3-1 for the order of electrodes. The lower 5-8 cm of each electrode was packed in soil; the upper part and wire lead were left exposed. The equipment base was located next to the control vault, approximately 30m north of well 1 (and hole 15). A transmission wire was dragged from the equipment base to each station hole. For the more distant stations, lengths of wire were spliced together. After layout, the wires were tested in pairs for breaks, using the hand-held digital multimeter (DMM); resistance values for all wires were found to be acceptably low. Each transmission wire was connected to the electrode lead using either a splice or alligator clips, then bound with electrical tape. Next, the transmission wires were connected to the terminals of the tie-in block.

At this point (~8 pm), with all wires and electrodes connected, the voltages were measured at the tie-in block using the DMM; the readings were roughly consistent with the previous survey at this site (3/99). As it was well past sunset at this point, activities were suspended for the night.

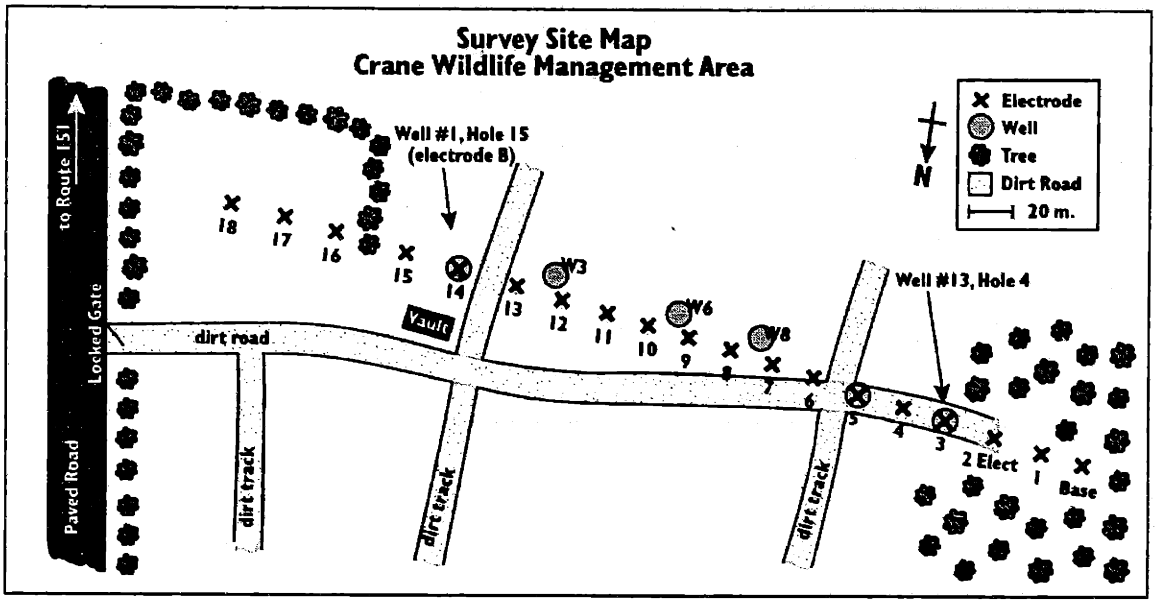

Figure 4-1: Map of survey site, showing electrode station positions relative to extraction wells and other features (scale is approximate)

4.2 Measurements Before, During, and After Shut-Off

At about 7:30 am, another set of voltage readings was taken with the DMM at the tie-in block terminals; these were reasonably consistent with the readings from the previous evening, though generally lower. A visual check was performed to verify the integrity of the wiring connections, and some electrical tape insulation was added to insure separation between channels at the tie-in terminals.

At 8 am, the pumps at all of the extraction wells were turned off by remote control; this was confirmed by a visual check of the gauges in the control vault. Starting at 9 am and approximately every 30 minutes thereafter, voltage measurements were taken with the DMM; it took 3-5 minutes to record the voltage readings of all 18 measurement electrodes.

The well pumps were turned back on by remote control at approximately 5:30 pm. More DMM readings were taken at ~30 minute intervals until 7:40 pm. After the last set of readings, the DAQ system was used to examine each channel's frequency response; the RMS voltages at DC and 60 Hz are shown in Table 9-3 and Figure 4-1.

At about 8:30 pm, all data collection ceased. The electrodes were retrieved, transmission wires were reeled in, and all the gear was packed up.

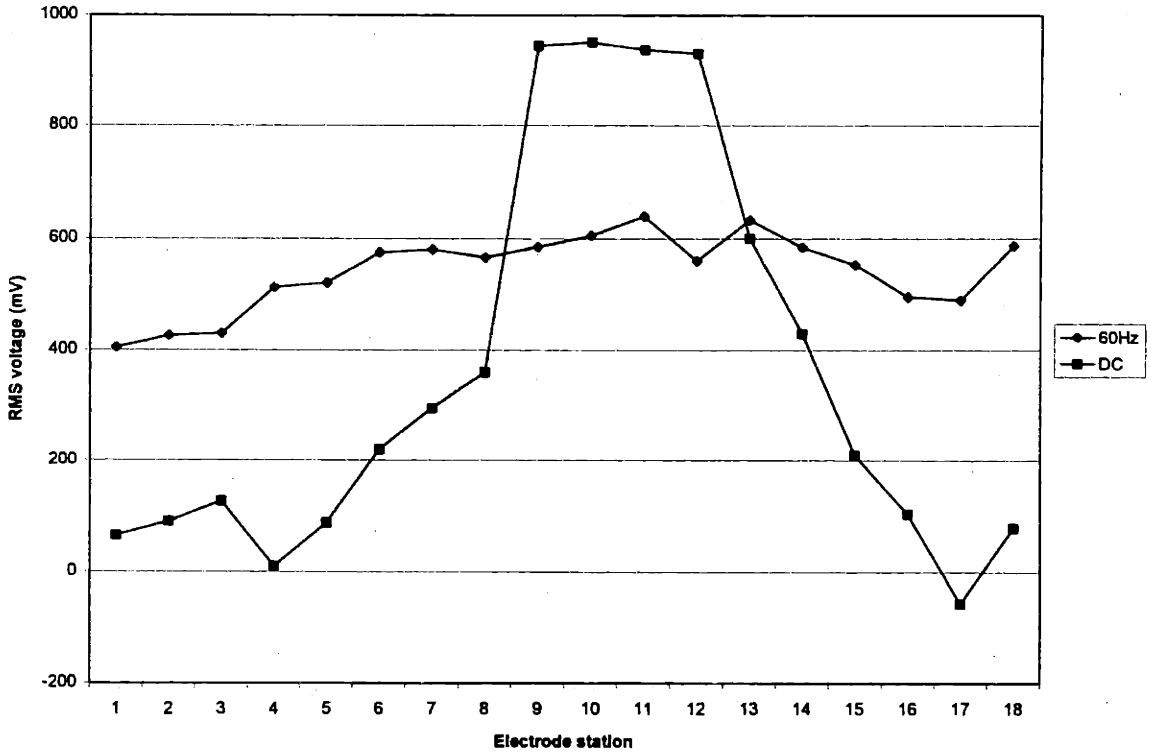

Figure 4-1: Unfiltered DAQ SP components (after turn-on, ~8:30 pm); electrodes are 20m apart.

5 RESULTS

In the field, all voltages were measured with respect to the reference/base electrode, which was located at the western end of the array, as previously described. As such, each of these SP measurements is the "integral" or sum of the SP voltages ("gradients") between consecutive intervening electrodes; for example, the measured SP integral between the reference electrode and electrode 2 is the sum of the SP gradient between the reference electrode and electrode 1 plus the SP gradient between electrode 1 and electrode 2.

Table 9-1 lists the SP integral readings taken manually with the hand-held digital multimeter (DMM) before shutoff, during the shutoff period, and after the well pumps were turned on again.

In Figure 5-1, the voltages measured for electrodes 9-12 are plotted over time; the down arrow indicates the approximate time at which the well pumps were turned off (8 am), while the up arrow indicates the approximate time at which they were turned on again (5:30 pm). Note that the time intervals between points are not equal, particularly at the start. Except for the first two points (before shut-off), the trend for each electrode shows a consistent, gradual decline of 15-30 mV up to the turn-on time; after turn-on, a consistent and gradual increase is seen for electrodes 9 and 10, while 11 and 12 are fairly flat (except for the anomalous readings at 5:30 pm). The SP integral plots for the other electrodes in the array (not included here) look similar, though at other absolute voltage levels. This trend is consistent with the behavior predicted by streaming-potential models, as will be discussed further on in section 6.

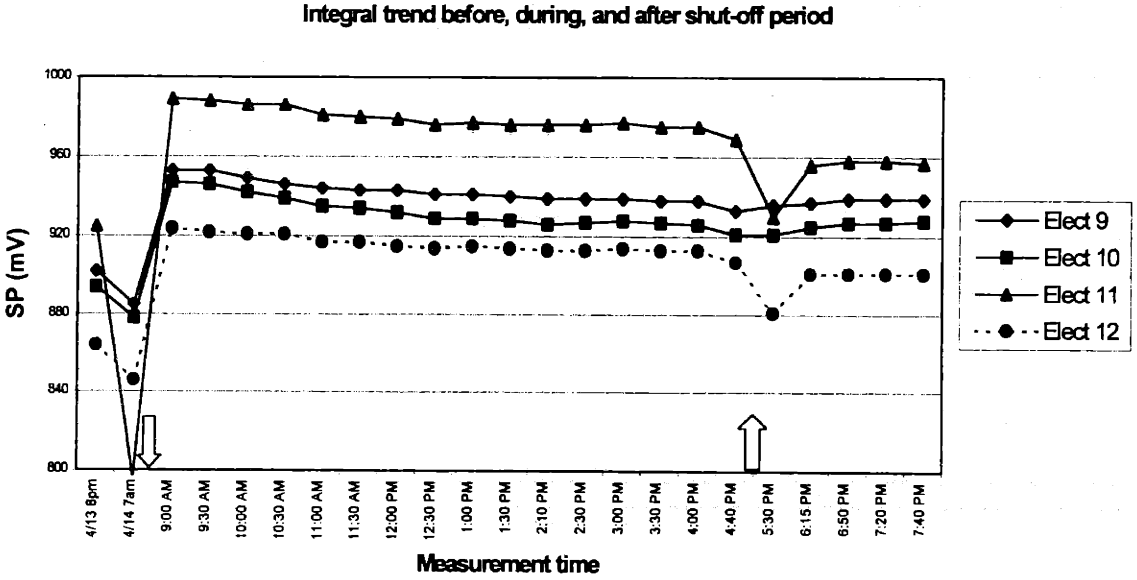

Figure 5-1: SP integral measurements for 4 electrodes near center of array; arrows show approx. shut-off and turn-on times

Figure 5-2 shows the voltage gradient (change to the specified electrode from the next lower-numbered one) across the array, at four different measurement times, two before shut-off and two after shut-off; each series of points represents the readings at a particular time. The block arrows indicate the approximate relative position of the active wells; the height of the arrows indicates the relative flow rate while pumping. The peak gradient voltage is at electrode 9, in the vicinity of the two highest-flow wells (6 and 7, each at 20 gpm). Electrodes 1-4 show a relatively high amount of fluctuation, in the range of 20-80 mV; possible causes are discussed in the next section. Electrodes 11 and 12 show an anomalous change (over 100 mV) at the 7am readings, but are otherwise consistent over the time interval.

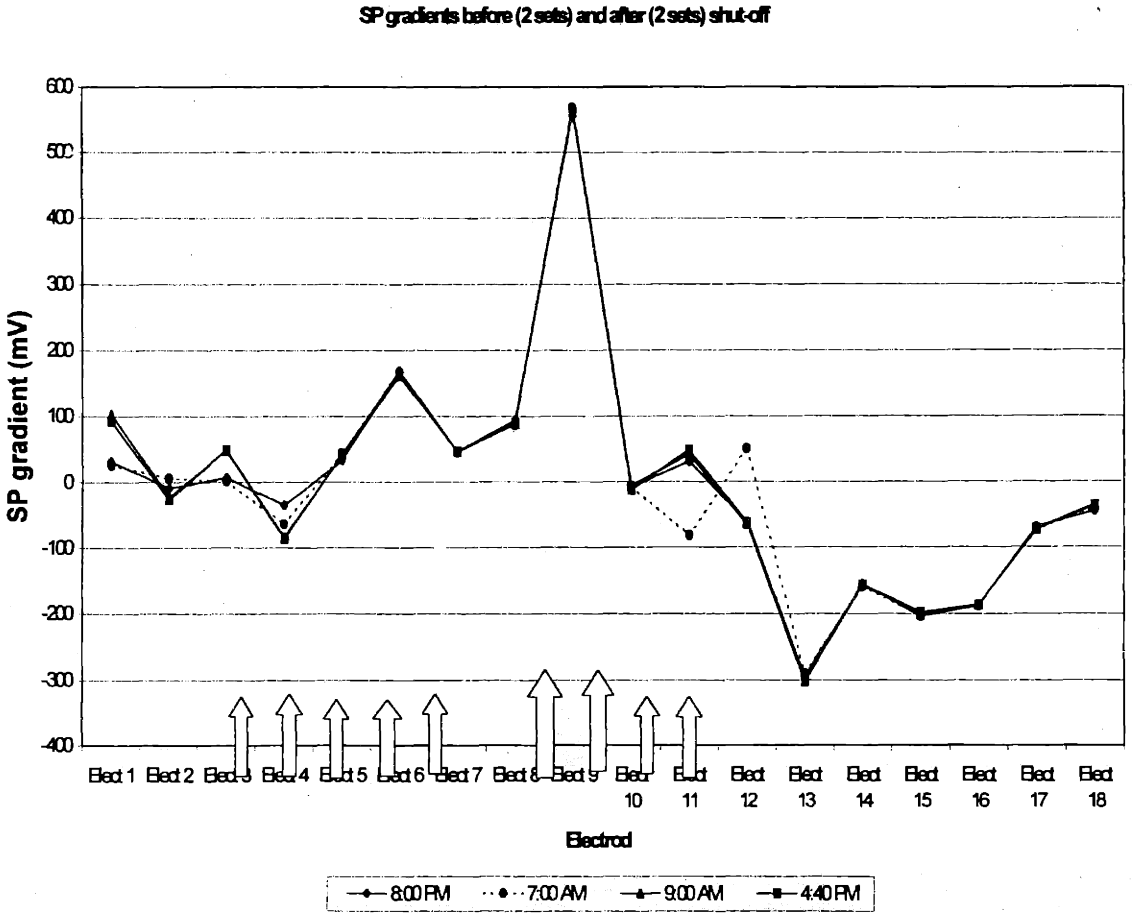

Figure 5-2: SP gradients (positive toward increasing electrode number)

The SP gradient trend for electrode 9 during the period before and during shut-off is shown in Figure 5-3. This electrode's trend was chosen for display because of its important location (at the center of the survey line, and near the two highest-flow wells), and because it registered the highest gradient magnitude. Except

for the first pre-shut-off point (8 pm), a gradual and steady decline in the gradient is clearly discernible. This matches the trend seen in the SP integral readings (Figure 5-1).

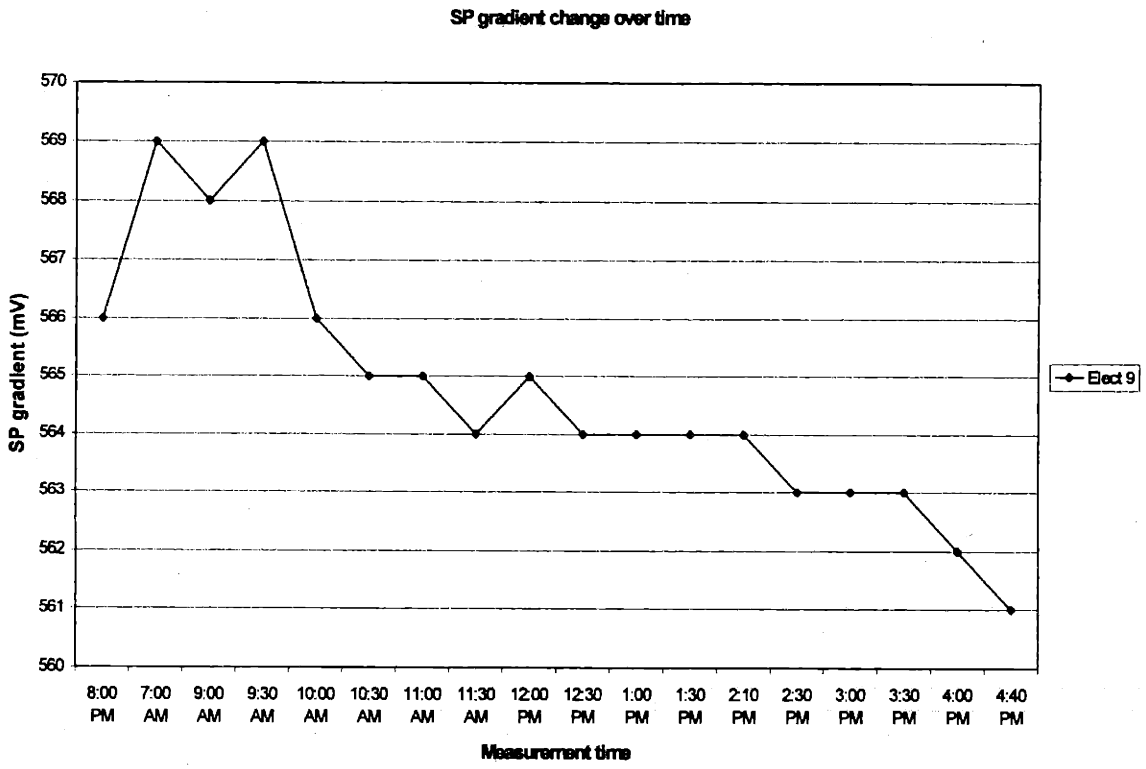

Figure 5-3: SP gradient trend over time for electrode 9

Because the gradient trend over the survey line (Figure 5-2) shows relatively high stability over time at the eastern end (electrodes 14-18), this end is likely to be a better starting point for an integral plot than the western end, which shows a high degree of fluctuation. Significant SP fluctuation near the starting point of an integral line tends to mask variations of interest farther along the line. Accordingly, the SP integrals before and during the shut-off period were recalculated using electrode 18 as the starting point, and summing the reversed gradients toward the base electrode (0); these values are shown in Table 9-2, and plotted in Figure 5-4 with one series of points for each measurement time. Note that the value at each electrode station is the sum of the gradients from all the higher-numbered electrodes; the integral value at electrode 18 is defined to be 0. Except for the anomalous points at 7 am at electrodes 10 and 11, the integral values from electrode 18 to electrode 5 are relatively stable over the survey period.

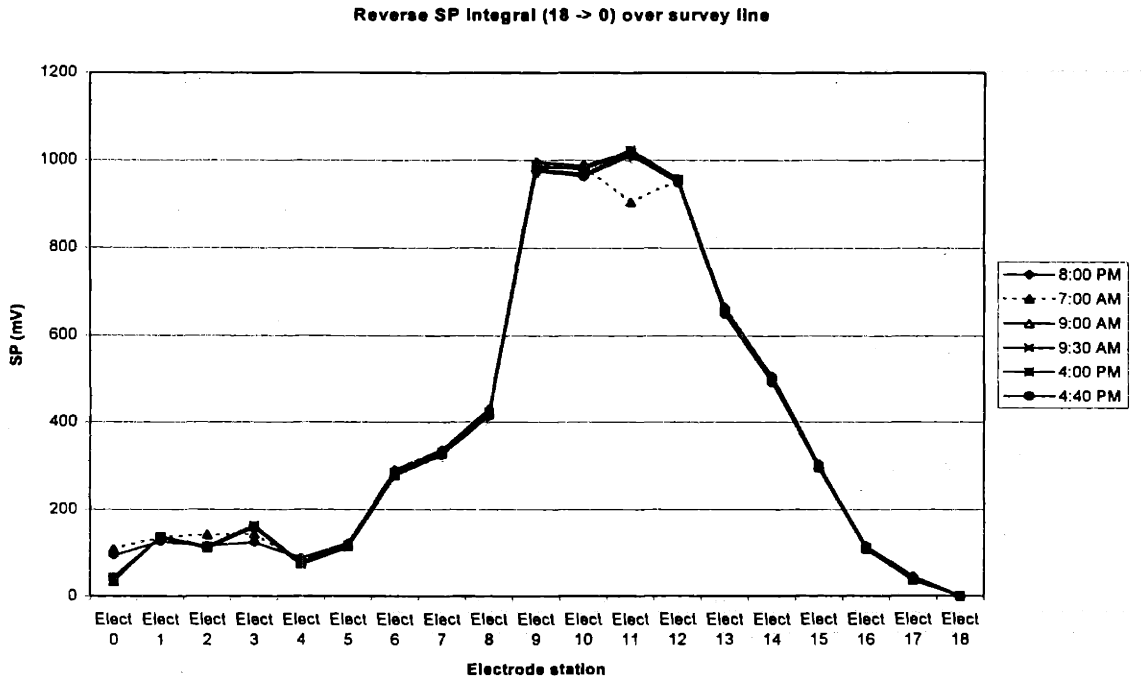

Figure 5-4: SP integrals starting at electrode 18, over time; values between 9:30am and 4:00pm closely match times shown.

Finally, to obtain a measure of the change in the SP values from the full-flow state (before shut-off) to the end of the shut-off period, the reverse-integral values (as described above) at 4:40pm were subtracted from the average of those at the two pre-shut-off measurement times (8pm and 7am). Because those pre-shut-off series diverge significantly at some of the electrodes, another integral difference was calculated using only the 8pm values, which appear to be more consistent with the post-shut-off measurements. The two integral difference sets are plotted in Figure 5-5. Once again, except for electrodes 0-4 and 11, the two difference sets are in close agreement (within 2 mV).

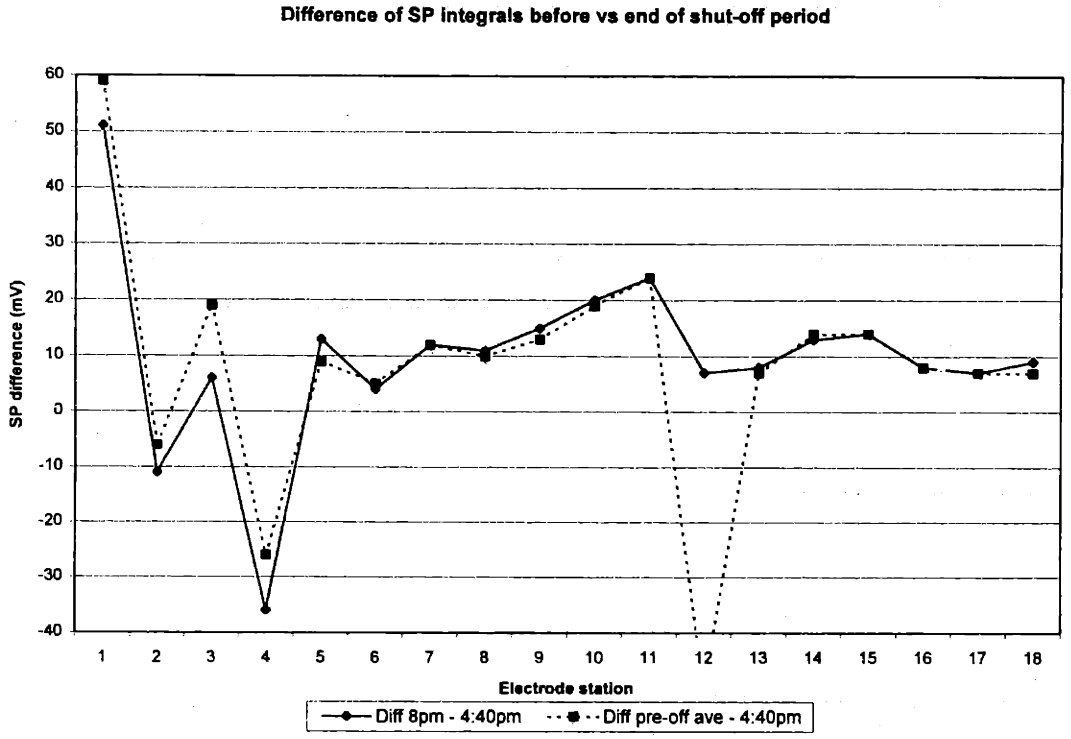

Figure 5-5: Difference of SP reverse integrals, from before shut-off to near end of shut-off period. Dashed line shows average of 8pm and 7am integral values; solid line uses only 8pm values.

6 ANALYSIS AND DISCUSSION

6.1 Correlations between SP Variations and Physical Features/Processes

As previously discussed in section 3.1, self-potential anomalies can be caused by a variety of processes involving the underground movement of charged ions. At this site, a number of different factors may contribute to SP variations, but two are particularly conspicuous: water flow induced by the extraction wells, and electrochemical diffusion due to the contaminant plume. To assess the contribution of water flow to the SP anomaly, it is necessary first to correlate the locations and changes in flow to the observed voltages.

While the extraction well pumps are in operation, water flows toward the wells from the surrounding aquifer medium. As first described by Helmholtz (Kruyt, 1952), negative charge flows in a direction opposite to the capillary fluid flow. Because negative charge moves from an area of higher potential to one of lower potential, the resulting "streaming" potential difference must be positive in the direction of flow, which is to say toward the extraction wells. Superficially, this would seem to be supported by the gradients shown in Figure 5-2, before and at the start of the pump shut-off: electrode stations 13-18, which are far from any active well, show a negative SP gradient, possibly indicating water flow away from their vicinity; while electrode stations 5-10, located near the active wells, show positive SP gradients, suggesting water flow toward their vicinity. The unusually high gradient at electrode station 9 is particularly suggestive, because this station was located between the two wells with the highest flow rate (6 and 7). However, the high fluctuation at electrodes 1-4 is puzzling, as is the negative gradient at electrode 4, which lies between two active wells (12 and 13); clearly these cannot be explained by pumping flow alone. A likely explanation is the close proximity of trees to these electrodes (see Figure 4-1); tree root systems cause near-surface water flow and variations in soil chemistry, which may generate significant potential variations over time and short distances.

When the pumps were shut off, water ceased to flow out of the wells (Davis et al, 1999). The resultant drop in suction pressure would have gradually decreased the flow rate in the surrounding rock medium. In turn, the streaming potential would have steadily decreased (see the mathematical derivation in the next section). This process correlates well to the trend seen in Figure 5-1 and Figure 5-3. However, the disparities between the two sets of measurements before shut-off (4/13 8pm and 4/14 7am) are difficult to explain; one possible cause is tellurics, long-period and long-wavelength SP variations due to fluctuations in the Earth's magnetic field.

The magnitude of the decrease in the streaming potential after shut-off is also expected to vary with proximity to active wells; as will be seen in detail in the next section, the electrodes nearest to the active wells should show the greatest decrease, while the stations farthest away should show little or no decrease in SP. This is supported by Figure 5-5, though not as strongly: as expected, electrodes 6-10 had a higher change than electrodes 15-18; however, electrodes 6 and 7, which were located near active wells, had an SP change similar to that of wells 13 and 14, which were farther away from any active wells. So it seems that

simple proximity is not sufficient to account for the magnitude of SP changes during shut-off. It is possible that non-uniform flow patterns, local gradient variations, or other aquifer features may have affected the observed SP magnitude changes.

6.2 Model of Streaming Potential

As originally formulated by Helmholtz and others (Kruyt, 1952), the convective current due to streaming potential in capillary flow can be expressed as follows:

$$I_{conv} = \frac{\pi a^2 \varepsilon \zeta \Delta P}{\eta \Delta l}$$

a = capillary radius, ε = dielectric permittivity of liquid, ζ = zeta potential, η = viscosity,

ΔP = change in pressure over distance Δl

The "zeta potential" is defined as the potential difference between the fixed and flowing layers of fluid in the slipping plane at the capillary wall (Overbeek, 1952).

The volume flow rate can be expressed as:

$Q = \frac{\pi a^4}{8\eta} * \frac{\Delta P}{\Delta l}$, which can be rearranged as: $\frac{\Delta P}{\Delta l} = \frac{8\eta Q}{\pi a^4}$

then substituting into the convection current equation above:

$$I_{conv} = \frac{\pi a^2 \varepsilon \zeta}{\eta} * \frac{8\eta Q}{\pi a^4} = \frac{8\varepsilon \zeta Q}{a^2}$$

The hydraulic permeability of a capillary can be expressed as:

$k = \frac{a^2}{8}$ with units of Darcys or m^2

substituting into the convection current equation:

$$I_{conv} = \frac{8\varepsilon \zeta Q}{8k} = \frac{\varepsilon \zeta Q}{k}$$

We assume that this expression also applies to a uniform porous medium, such as an idealized aquifer sediment.

For water, $\varepsilon = 80*(8.854*10^{-12})$ F/m

The zeta potential of the aquifer sediments is estimated to be in the range of 0.03-0.08 V (Morgan, 1989); a nominal value of 0.05 V is chosen for this model.

The hydraulic conductivity of the aquifer sediments at the remediation site has been determined to be 169 ft/day (ABB, 1992 and Davis, 1999).

Using the following conversion formulas: 10^8 Darcy = $3.22*10^3$ ft/sec , 1 Darcy = 10^{-12} m^2

the hydraulic permeability is calculated at 60.7 Darcys or $6.07*10^{-11}$ m^2

Next, the voltage potential generated at each measurement electrode is computed from an I_{conv} source taken to be at the top of the intake screen of each well; for all the extraction wells, the depth of the top of the intake screen is 128 ft (39m). For a surface potential V due to an underground point current source I at depth z, across a distance d through a medium of uniform resistivity ρ, the formula is (Telford, 1990):

$$V = \frac{I \cdot \rho}{4\pi \cdot d}$$

The resistivity in the area at depths of 100-150 ft has been measured at approximately 10^4 ohm-meters (ERL, 1994).

However, this formula applies only if $d \leq z$, meaning the receiver is directly above the current source.

If $d >> z$, then the following half-space formula applies:

$$V = \frac{I \cdot \rho}{2\pi \cdot d}$$

For $d > z$, the voltage can be calculated by an interpolation between the above two formulas.

Because the actual aquifer sediments at this site are not an ideal homogeneous medium, and the resistivity at extraction depth is not precisely known, some variation in the resistivity and current source depth should be taken into account when computing the streaming potential voltage. The source depth may range along the length of the intake screen, 39m – 42m, if there is blockage at the top of the screen. The sediment resistivity may be taken to vary from $0.5*10^4$ to $2*10^4$ ohm-meters. Using these ranges, and the estimated range for zeta potential, a streaming potential range for each well can be calculated.

Table 6-1: Ranges of values for loosely-constrained parameters in streaming-potential model

	Minimum	Maximum	Nominal
Zeta Potential (volts)	0.03	0.08	0.05
Streaming Current for 15 gpm well (amps)	$3.3*10^{-4}$	$8.8*10^{-4}$	$5.5*10^{-4}$
Streaming Current for 20 gpm well (amps)	$4.4*10^{-4}$	$1.2*10^{-3}$	$7.4*10^{-4}$
Resistivity (ohm-meters)	$0.5*10^4$	$2.0*10^4$	$1.0*10^4$
Depth of source (meters)	39	42	40

Table 9-4 shows the distance calculated from each measurement electrode to the top of each active extraction well. Table 9-5 shows the modeled potential at each electrode due to each well, using the mean values for resistivity, depth, and zeta potential described above; and the minimum and maximum total potential at each electrode from all the wells, based on the likely range limits of those parameters.

6.3 Comparison of Field Results to SP Model

A theoretically sound way to determine the streaming (electrokinetic) potential component of the full-flow (before shut-off) measurements is to extrapolate the trend in shut-off period readings to infinity, then subtract the minimum values from the full-flow measurements. Cessation of pumping is expected to produce an exponential decay in the flow rate at the well bottom, to the natural aquifer flow rate (negligible for SP considerations).

To obtain the minimum voltage at each electrode, a curve-fitting program was used to fit the shut-off period measurements with an exponential-decay curve of the form:

$V = B_0 + B_1 * e^{(-C*t)}$

B_0+B_1 is the full SP anomaly at the moment the pumps are shut off; B_0 is the steady-state no-flow SP anomaly at infinite time (if the wells remained off); B_1 is the streaming-potential component at full-flow. The intent was to find these constants for each electrode station, from 16 sets of readings during the shut-off period. Because the gradient values for many of the stations show only negligible variations (0-1 mV) during most of the period, it is difficult to accurately fit them with exponential-decay curves; instead, the integral values were fitted, as they show a more significant and consistent pattern of decrease. Weighting was equal for all data points. For each electrode station, a few seed values were tried, and the curve fitting was iterated until a stable RMS error was obtained. Table 6-12 shows the B_0, B_1, C, and RMS error values obtained for each electrode station.

Table 6-2: Exponential-decay fit constants for SP integrals during shut-off

Electrode station	B_0	B_1	C	RMS error
1	86	18	0.15	1.3
2	63	21	0.19	0.5
3	112	22	0.24	0.8
4	28	21	0.33	0.9
5	70	22	0.39	1.1
6	232	26	0.28	0.6
7	279	22	0.19	0.7
8	371	17	0.21	0.9
9	930	27	0.19	1.3
10	919	37	0.26	1.5
11	968	27	0.2	1.7
12	908	20	0.22	1.4
13	606	19	0.19	1.2
14	451	21	0.42	1.1
15	251	16	0.25	0.9
16	61	18	0.21	0.9
17	-9	16	0.26	0.9
18	-44	17	0.47	0.9

The next two figures show four data sets that may be indicative of the streaming potential component of the SP anomaly. In Figure 6-1, the difference in SP gradients between pre-shut-off (8pm) and end of shut-off period (4:40pm) measurements, vs. the modeled voltage potential gradients from Table 9-5. While the shapes of the two curves don't quite match, the absolute values are within 10 mV except for electrodes 1-4. Figure 6-2 shows two other perspectives of streaming potential: the difference in SP integrals between those two measurement times (as in Figure 5-5), and the exponential-decay fall-off of the integral measurements during the shut-off period (the value of B_1 from Table 6-12). As expected, the shape of the latter data set (exponential decay) closely resembles the former, but it is smoother and its magnitude is higher. This correlation lends credence to the exponential-decay fit method of assessing the streaming potential; because the magnitude of the measured difference may have been reduced by telluric variation or other factors not of interest, it can be assumed that the exponential-decay fit values are a more valid approximation of the actual streaming-potential fall-off.

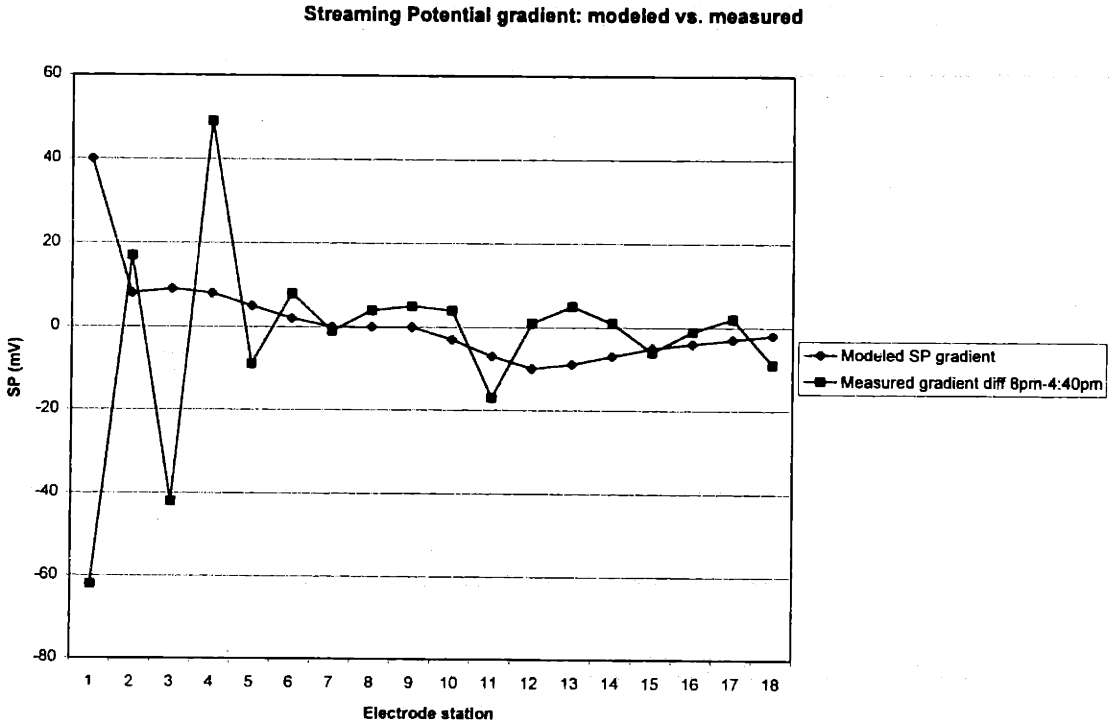

Figure 6-1: Streaming potential gradients, modeled vs. measured difference over shut-off period

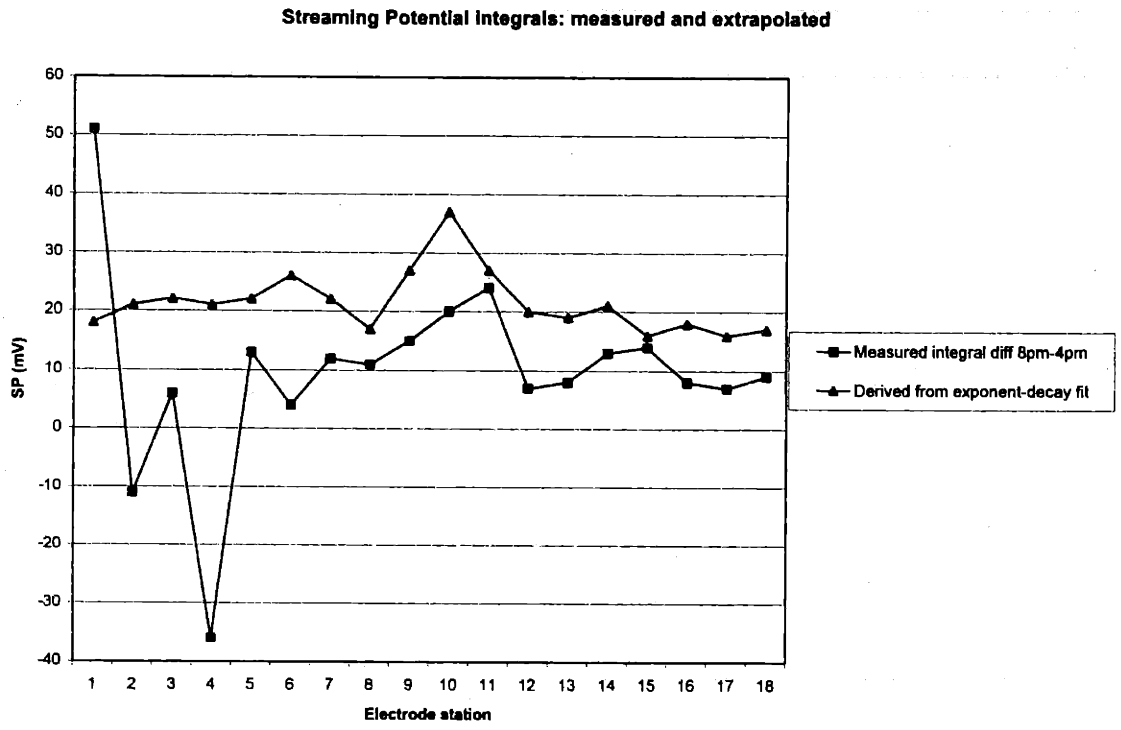

Figure 6-2: Streaming potential integrals starting at electrode 18; measured difference during shut-off period vs. extrapolated from exponential-decay curve fitting.

A final comparison is made in Figure 6-4 between the exponential-decay fit values (as seen in the previous figure) and the minimum modeled streaming-potential values (using the minimum values of resistivity and zeta potential, and the maximum depth, from Table 6-1). The fairly close correlation in both shape and magnitude between the two curves is likely to be more than coincidence. Pending further field study, this can be taken as a more precise indication of the probable values of resistivity and zeta potential at this site. The disparities may be due to heterogeneity in flow or resistivity; at the peripheral electrodes, the higher-than-modeled values suggest the flow extent beyond the line of extraction wells. It should also be noted that the point-source current model used here is a simplification of the currents generated by the actual flow patterns at the site.

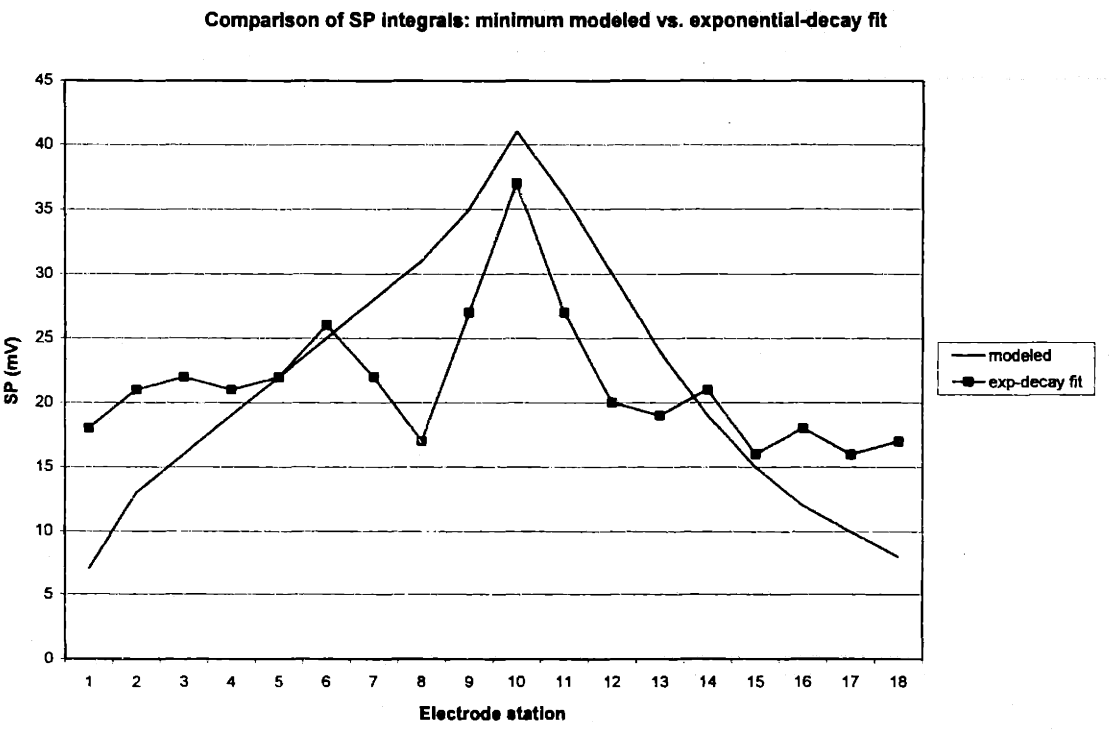

Figure 6-4: Streaming potential integral comparison: exponential-decay fit vs. modeled minimum

6.4 Uncertainties and Possible Sources of Error

As in any field investigation, a number of sources of possible error or uncertainties may have affected this survey. Some of these are general to self-potential survey methods, while others are particular to the way in which this investigation was conducted. Here they are presented in two categories: systematic and random errors.

6.4.1 Systematic Errors

Natural and artificial sources of noise that commonly plague SP surveys are likely to have been present. Though there exist established techniques for assessing and eliminating such noise sources from measurements (Corwin, 1990), those techniques were not employed due to various limitations.

First, a consideration of natural sources. Telluric currents, caused by variations in the Earth's magnetic field, may have produced long-period, long-wavelength fluctuations in the SP measurements; in particular, they may be partly or entirely responsible for the variation seen between the two sets of readings before shut-off (4/13 8pm and 4/14 7am), because these measurements were taken at least 11 hours apart. If this was the case, then the potential change during the 9 hours or so of the shut-off period would also have been affected by telluric variation; though it is difficult to gauge the sign and magnitude of the effect.

Perhaps less significantly, local variations in topography and near-surface geology may have caused some spatial variation across the survey line. Because these aspects were not mapped, it is not currently possible to assess their impact on the SP measurements.

Turning to artificial sources of noise, the most significant suspect is stray DC currents, primarily from grounded electrical equipment. The equipment used to power, control and monitor the extraction pumps is likely to have produced ground currents, probably even during the shut-off period. Under the survey conditions, a complete cessation of electrical activity involving this equipment was not feasible. In addition, there is a possibility that the automated data-acquisition system (DAQ) which was used during the survey (with disappointing results) may have caused a ground current loop.

Another source of artificial noise is provided by the corrosion of buried metal. The extraction wells, monitoring wells, and water pipes all have metal components that are progressively corroded. The oxidation-reduction reactions involved in the corrosion process generate a weak current, which near the surface can produce measurable potentials. To gauge the magnitude of these redox potentials, the locations and corrosion rates of the wells and pipes would need to be ascertained, and a corrosion-current model constructed; this has not yet been done.

The cumulative impact of these systematic noise sources (exclusive of temporal variations) could be accurately determined through a resistivity survey of the site. While this had been planned, it was omitted due to limitations on time and resources.

6.4.2 Random Errors

A few non-reproducible phenomena may have compromised the SP measurements. The most likely one is electrode polarization drift. While the initial polarizations of the measurement electrodes were measured 1 day before the survey (Table 3-1), they were not subsequently retested for polarization drift; this was due partly to oversight and partly to time constraints during the survey. Owing to deterioration from age and wear, some of the electrodes may have leaked electrolyte fluid at a higher rate than desired, which might have caused a significant amount of polarization drift. Mistakes made in preparation of the electrodes (use of tap water instead of distilled, omission of recoating with AgCl) are likely to have exacerbated the polarization drift. Temperature variations during the survey might also have contributed to drift, considering that the electrodes were emplaced for more than 24 hours.

Another possible cause of random error is disturbances to the electrode environment. The electrodes and transmission wires were vulnerable to animal activity, both localized (worms, burrowing rodents) and roaming (dogs, horses, coyotes, etc); several of the latter were observed in the area during the survey. While a few periodic visual checks were made of the electrodes' physical integrity, it is possible that a subtle animal disturbance may have affected the performance of one or more electrodes. There is also the chance of improper connections, either between an electrode and the surrounding soil, or between a transmission wire and an electrode lead (which might have been inadvertently grounded).

Finally, the quickness of voltage readings may have been an issue. Because many electrodes had to be measured at each sampling time, only a few seconds were spent waiting for each electrode's reading to stabilize (between connecting the voltmeter and recording the value). This may not have been sufficiently long for some of the electrodes, so a transient value might have been recorded instead of the steady one. However, this is less likely, in view of past experience at this site, and the observed stability of voltage readings.

Finally, random human errors may have occurred in processing of the collected measurements after the survey, in transcription of the data or input to calculations.

6.5 Possible Explanations for SP Anomaly Magnitude

A case has been made in previous sections for an apparent 10-40 mV contribution to the observed SP from streaming potential due to the operation of the extraction wells; the actual magnitude of this streaming potential may be higher or lower, depending on the effect of the sources of error and uncertainty described above. However, this doesn't explain the distinct, stable, and extremely high SP gradients measured at electrodes 9 and 13, among others (see Figure 5-2). The gradient at electrode 9 (actually, between 8 and 9) is particularly intriguing, because it matches the measurement made at that approximate spot in an earlier SP survey with a different methodology (March 5, 1999; results unpublished, not shown here). As this particular SP anomaly seems to have persisted between surveys over one month apart, random errors and noise sources can be ruled out. One or more of the systematic errors listed earlier are likely to be

responsible; probably a stray ground current from the electrical pumping equipment, or near-surface corrosion of the nearby wells and pipes. Another possible cause, though much less likely, is an electrochemical potential due to the groundwater contaminant plume; however, it seems improbable that such a sharp transition and high potential would be due primarily to a chemical concentration gradient, judging from past studies of the SP effects of contaminant migration.

To solve this mystery, two steps would be most useful in the next survey: to precisely map the location, depth, and corrosion rate of all buried metal between and near electrode stations 8 and 9; to shut off all electricity to the pumping equipment while the SP measurements are taken. In this way, the two most likely sources of noise could be isolated and accounted for.

7 CONCLUSIONS

As detailed in the preceding sections, proper interpretation of the collected data was hampered by several factors, including systematic and random errors, some key omissions in methodology, and the inability to isolate potential noise sources. Nevertheless, a few significant correlations have been identified, suggesting some partial answers to the questions posed in the introduction in regard to the subsurface water flow. First, the resemblance between the graphs of the measured change in the SP integral over the shut-off period and the drop-off given by the exponential-decay fit to the measured values confirms the probable validity of the exponential-decay fit derivation as an indicator of the streaming-potential component. Second, the comparison of the exponential-decay drop-off values to the modeled values based on point-source currents shows a significant similarity, particularly near the center of the well fence; the overlaps suggest that the resistivity and/or zeta potential values may be at the lower end of the predicted range, while the divergences might indicate non-uniform flow or resistivity conditions. In particular, the higher-than-modeled SP drop-offs beyond the ends of the well fence suggest that, during extraction pumping, significant flow may extend beyond the measurement stations used in this survey. Thus, the zone of water flow has not been clearly delineated, and may extend farther than previously thought.

To better assess the water flow extent and resultant streaming potential, a future SP survey would need to transcend the problems and limitations of this one. In addition to avoiding the errors and omissions described earlier (in regard to electrode preparation, polarization measurement, etc), some additional steps would be useful. The survey line should be extended farther in both directions, to increase the probability of spanning the flow zone. A second, perpendicular survey line should be laid out and measured concurrently, to determine SP changes up- and down-gradient. A resistivity survey should be conducted at the well fence, to better gauge the resistivity magnitude at the extraction depth and to map out non-uniform spatial variations. The shut-off time period should be extended, to more accurately measure the temporal changes, account for telluric variations, and allow better exponential-decay curve fitting. If possible, all grounded electrical equipment at the site should be turned off during the measurement period, to reduce noise from stray DC currents.

The analysis shows that the streaming potential component, due to water flow during extraction pumping, comprises only a small part (<50 mV) of the total SP anomaly measured along the well fence (e.g. >500 mV in the vicinity of well #7); the bulk of the anomaly must be due to other sources. Some of the suggested steps outlined above would help to isolate some of the uninteresting noise sources (stray DC currents, corrosion redox), and allow assessment of the contribution from chemical concentration gradients, including the contaminant plume. In this way, the ultimate goal of this investigation might be attained: a delineation of the contaminant plume, and comparison to the effective extraction flow zone.

8 REFERENCES

ABB Environmental Services, Inc. Groundwater Focused Feasibility Study: West Truck Road Motor Pool (AOC CS-4). February, 1992.

Corwin, R.F. "The Self-Potential Method for Environmental and Engineering Applications". Geotechnical and Environmental Geophysics, Review and Tutorial; Society of Exploration Geophysicists Investigations in Geophysics, Vol. 1, No. 5, 1990.

Davis, B., Galant, J., and Forbes, R. IRP staff. Personal discussions, 1999.

ERL (Earth Resources Laboratory) course 12.214: Environmental Geophysics. Geophysical Study of Contaminant Spill CS-4 at Otis Air Base. Massachusetts Institute of Technology: Cambridge, 1994.

Mackay, D.M. and Cherry, J. "Groundwater contamination: pump-and-treat remediation". Environmental Science Technology, Vol. 23, No. 6, 1989.

Morgan, F.D., Fundamentals of streaming potentials in geophysics: Laboratory methods, in *Lecture Notes in Earth Sciences*, 27, S.Bhattacharji, G.M. Friedman, H.J. Neugerbauer and A. Seilacher (eds.), Springer-Verlag, 1989.

Overbeek, J.Th.G. "Electrokinetic Phenomena". Colloid Science, ed. Kruyt, H.R. Vol. 1, Elsevier Publishing, 1952.

Telford, W.M., Geldart, L.P., and Sheriff,R.E. Applied Geophysics, 2nd edition. Cambridge University Press, 1990.

Vichabian, Y. An Environmental Application of Self Potential Geophysics. M. Eng Thesis, Department of Civil and Environmental Engineering, Massachusetts Institute of Technology: Cambridge, 1997.

9 APPENDIX

Table 9-1: SP Integral measurements recorded in field (split across two tables)

Integral	Elect 1	Elect 2	Elect 3	Elect 4	Elect 5	Elect 6	Elect 7	Elect 8	Elect 9
Polarizatio	-5	2	0	2	1	2	-1	-3	2
4/13 8pm	26	24	29	-4	28	198	241	333	904
4/14 7am	21	34	34	-28	14	182	224	313	887
9:00 AM	98	82	128	44	85	253	296	382	955
9:30 AM	97	81	128	44	84	252	295	381	955
10:00 AM	95	80	126	41	82	250	293	380	951
10:30 AM	93	78	124	39	80	247	291	378	948
11:00 AM	90	76	121	37	77	245	289	376	946
11:30 AM	90	75	120	36	76	243	288	376	945
12:00 PM	89	74	120	36	76	243	288	375	945
12:30 PM	89	73	119	35	75	241	287	374	943
1:00 PM	89	73	118	34	74	240	286	374	943
1:30 PM	88	72	117	33	73	239	285	373	942
2:10 PM	88	71	116	32	73	239	284	372	941
2:30 PM	89	71	116	32	73	239	285	373	941
3:00 PM	88	70	116	32	72	238	284	373	941
3:30 PM	87	69	116	31	71	237	283	372	940
4:00 PM	87	69	115	31	71	237	284	373	940
4:40 PM	88	69	116	34	75	237	281	369	935
5:30 PM	88	69	117	36	77	238	284	372	938
6:15 PM	89	70	117	36	78	239	284	373	939
6:50 PM	90	71	119	38	79	240	285	373	941
7:20 PM	91	71	119	38	80	241	286	374	941
7:40 PM	91	71	118	37	79	241	286	374	941

Elect 10	Elect 11	Elect 12	Elect 13	Elect 14	Elect 15	Elect 16	Elect 17	Elect 18
2	0	2	0	-2	-5	2	2	-2
896	925	866	569	411	204	23	-47	-96
880	796	848	556	395	188	7	-66	-111
949	989	926	622	463	258	78	5	-36
948	988	924	621	462	258	79	4	-37
944	986	923	620	459	255	74	3	-39
941	986	923	618	457	254	74	0	-40
937	981	919	615	453	251	72	-2	-44
936	980	919	615	454	252	71	-2	-44
934	979	917	615	453	251	71	-2	-43
931	976	916	614	453	251	71	-1	-43
931	977	917	614	453	251	70	-2	-44
930	976	916	613	452	250	69	-3	-46
928	976	915	611	451	248	68	-5	-46
929	976	915	612	452	249	68	-5	-46
930	977	916	612	452	249	68	-5	-46
929	975	915	612	450	249	67	-5	-46
928	975	915	612	451	249	67	-5	-45
923	969	909	607	448	247	67	-5	-45
923	930	883	605	447	248	69	-3	-44
927	956	903	610	450	250	70	-2	-41
929	958	903	611	450	250	70	-2	-41
929	958	903	612	449	251	71	-1	-40
930	957	903	610	447	250	70	-2	-41

Table 9-2: SP integrals corrected for initial polarization, and calculated starting at electrode 18 = 0

Reverse I	Elect 0	Elect 1	Elect 2	Elect 3	Elect 4	Elect 5	Elect 6	Elect 7	Elect 8
8:00 PM	94	125	116	123	88	121	290	336	430
7:00 AM	109	135	141	143	79	122	289	334	425
9:00 AM	34	137	114	162	76	118	285	331	419
9:30 AM	35	137	114	163	77	118	285	331	419
10:00 AM	37	137	115	163	76	118	285	331	420
10:30 AM	38	136	114	162	75	117	283	330	419
11:00 AM	42	137	116	163	77	118	285	332	421
11:30 AM	42	137	115	162	76	117	283	331	421
12:00 PM	41	135	113	161	75	116	282	330	419
12:30 PM	41	135	112	160	74	115	280	329	418
1:00 PM	42	136	113	160	74	115	280	329	419
1:30 PM	44	137	114	161	75	116	281	330	420
2:10 PM	44	137	113	160	74	116	281	329	419
2:30 PM	44	138	113	160	74	116	281	330	420
3:00 PM	44	137	112	160	74	115	280	329	420
3:30 PM	44	136	111	160	73	114	279	328	419
4:00 PM	43	135	110	158	72	113	278	328	419
4:40 PM	43	136	110	159	75	117	278	325	415

Elect 9	Elect 10	Elect 11	Elect 12	Elect 13	Elect 14	Elect 15	Elect 16	Elect 17	Elect 18
996	988	1019	958	663	507	303	115	45	0
994	987	905	955	665	506	302	114	41	0
987	981	1023	958	656	499	297	110	37	0
988	981	1023	957	656	499	298	112	37	0
986	979	1023	958	657	498	297	109	38	0
984	977	1024	959	656	497	297	110	36	0
986	977	1023	959	657	497	298	112	38	0
985	976	1022	959	657	498	299	111	38	0
984	973	1020	956	656	496	297	110	37	0
982	970	1017	955	655	496	297	110	38	0
983	971	1019	957	656	497	298	110	38	0
984	972	1020	958	657	498	299	111	39	0
983	970	1020	957	655	497	297	110	37	0
983	971	1020	957	656	498	298	110	37	0
983	972	1021	958	656	498	298	110	37	0
982	971	1019	957	656	496	298	109	37	0
981	969	1018	956	655	496	297	108	36	0
976	964	1012	950	650	493	295	108	36	0

Table 9-3: RMS voltage components of unfiltered SP integrals measured with DAQ system, after flow resumption (4/14 8:30pm)

Compone	Elect 1	Elect 2	Elect 3	Elect 4	Elect 5	Elect 6	Elect 7	Elect 8	Elect 9
60Hz	404	426	430	512	520	575	580	566	585
DC	65.5	91	127	10	88	220	295	360	945

Elect 10	Elect 11	Elect 12	Elect 13	Elect 14	Elect 15	Elect 16	Elect 17	Elect 18
605	640	560	633	584	553	495	490	587
951	937	930	600	430	210	105	-57.4	80

Table 9-4: Distances from each electrode to each active well's intake screen; column 2 shows the electrode station's distance from the reference/base electrode

Elect #	Elect dista	dist to w4	dist to w5	dist to w6	dist to w7	dist to w9	dist to w10	dist to w11	dist to w12	dist to w13
1	65	682.4954	623.6986	565.1548	506.9517	392.1734	336.1547	281.7801	230.2173	183.8478
2	130	618.8093	560.2901	502.1205	444.4378	331.5494	277.3536	226.1084	180.3469	145.3444
3	195	555.4278	497.2927	439.659	382.7532	272.9469	222.036	176.9181	143.1782	130
4	260	492.4683	434.885	378.0542	322.374	218.0023	173.5655	141.1559	130.0961	145.3444
5	325	430.1163	373.3631	317.805	264.1969	170.2939	139.2839	130.384	147.6482	183.8478
6	390	368.6801	313.2491	259.8557	210.0595	137.5682	130.8625	150.0833	187.4166	234.3608
7	455	308.707	255.5386	206.1553	164.0122	131.5295	152.6434	191.0497	238.5372	290.6888
8	520	251.2469	202.2993	161.0124	134.6291	155.3222	194.7434	242.7447	295.1694	350.0357
9	585	198.4943	158.1139	133.4166	133.4166	198.4943	246.9818	299.6665	354.683	411.0961
10	650	155.3222	132.382	134.6291	161.0124	251.2469	304.1792	359.3397	415.8425	473.2071
11	715	131.5295	136.0147	164.0122	206.1553	308.707	364.0055	420.5948	478.0167	536.0037
12	780	137.5682	167.1077	210.0595	259.8557	368.6801	425.3528	482.8302	540.8558	599.2704
13	845	170.2939	214.0093	264.1969	317.805	430.1163	487.6474	545.7105	604.1523	662.8725
14	910	218.0023	268.561	322.374	378.0542	492.4683	550.5679	609.0361	667.7762	726.7221
15	975	272.9469	326.9557	382.7532	439.659	555.4278	613.9218	672.6812	731.642	790.7591
16	1040	331.5494	387.4597	444.4378	502.1205	618.8093	677.5876	736.563	795.6915	854.9415
17	1105	392.1734	449.2215	506.9517	565.1548	682.4954	741.485	800.6248	859.8837	919.2388
18	1170	454.0099	511.7861	570.0219	628.5897	746.4081	805.5588	864.8266	924.1888	983.6285

Table 9-5: Modeled streaming potential (volts) at each electrode due to each active well's flow, using nominal parameter values; and sum of all voltage contributions, using minimum parameter values.

Elect #	V from w4	V from w5	V from w6	V from w7	V from w9	V from w10	V from w11	V from w12	V from w13	V sum min
1	0.000992	0.001201	0.001945	0.002398	0.002707	0.003341	0.004185	0.0051814	0.0063701	0.0070802
2	0.001227	0.018737	0.002425	0.00297	0.003421	0.0042351	0.0053046	0.0065172	0.0077799	0.0131541
3	0.001507	0.023373	0.003038	0.003738	0.004337	0.0053671	0.0065823	0.0079098	0.0087025	0.0161387
4	0.001881	0.028964	0.003825	0.004726	0.005494	0.0067248	0.0079767	0.0086849	0.0077799	0.019014
5	0.002358	0.036477	0.004839	0.005993	0.006796	0.0080965	0.0086421	0.0077129	0.0063701	0.0218211
6	0.002971	0.046147	0.006065	0.007585	0.008162	0.0085983	0.0075765	0.0063	0.0051207	0.0246315
7	0.00376	0.058534	0.007673	0.009445	0.00855	0.0075082	0.0061606	0.0050013	0.0040383	0.0276675
8	0.004714	0.07399	0.00954	0.011093	0.007366	0.006092	0.0048843	0.0039434	0.0031875	0.0312025
9	0.005955	0.091685	0.011274	0.011274	0.005955	0.0048268	0.0038968	0.0031136	0.0025261	0.0351267
10	0.007366	0.118695	0.011093	0.00954	0.004714	0.0038053	0.0030773	0.0024972	0.0020118	0.0406998
11	0.00855	0.104126	0.009445	0.007673	0.00376	0.0030061	0.0024405	0.0019893	0.0016101	0.0356501
12	0.008162	0.087203	0.007585	0.006065	0.002971	0.0024127	0.0019451	0.0015925	0.0013087	0.0298114
13	0.006796	0.069846	0.005993	0.004839	0.002358	0.0019234	0.0015579	0.0012808	0.0010567	0.0239127
14	0.005494	0.055155	0.004726	0.003825	0.001881	0.0015409	0.0012671	0.0010346	0.0008568	0.0189449
15	0.004337	0.044014	0.003738	0.003038	0.001507	0.0012401	0.0010237	0.0008392	0.0006975	0.0151087
16	0.003421	0.034819	0.00297	0.002425	0.001227	0.0010024	0.0008306	0.0006905	0.0005701	0.0119888
17	0.002707	0.027675	0.002398	0.001945	0.000992	0.0008136	0.0006766	0.0005645	0.0004725	0.0095611
18	0.002153	0.022106	0.001924	0.001567	0.000805	0.0006698	0.0005533	0.0004634	0.0003893	0.0076578